JOURNAL OF CATALYSIS 123, 463–476 (1990)

Steam Gasification of Graphite and Chars at Temperatures <1000 K over Potassium–Calcium–Oxide Catalysts

PEDRO PEREIRA, ROSEANN CSENCSITS, GABOR A. SOMORJAI, AND HEINZ HEINEMANN

Lawrence Berkeley Laboratory, Center for Advanced Materials, Materials and Chemical Sciences Division, 1 Cyclotron Road, Berkeley, California 94720

Received September 13, 1989; revised December 12, 1989

The catalytic steam gasification of graphite and several chars to H_2 and CO_2 has been studied using a K–Ca–O_x catalyst (K–Ca/C = 0.01 atomic ratio) in a flow reactor system at relatively low temperatures (600–950 K) and in a controlled atmosphere electron microscope (CAEM). A kinetic study of graphite gasification with water was performed. K–Ca–O_x appeared to be less sensitive to hydrogen partial pressure that has an inhibiting effect on this reaction than other active catalysts. Evidence was found for water dissociation on the catalyst. Activation energies obtained in the flow reactor system were essentially the same as those for graphite and chars and for various catalysts. The K–Ca–O_x catalyst was more resistant to sulfur poisoning than a K–Ni–O_x catalyst described in a previous publication. A CAEM study of the K–Ca–O_x-catalyzed steam gasification of graphite showed: (1) a homogeneous composition of the dispersed K–Ca catalyst mixture; (2) graphite consumption by edge recesssion during steam gasification; (3) an activation energy close to that found in the flow reactor system. The results indicate that steam gasification proceeds via water dissociation and oxygen transfer to the carbon. The rate-controlling step, however, is the C–C bond breaking next to a surface carbon–oxygen complex which produces CO_2. Chars gasify at rates higher by an order of magnitude than that of graphite. The K–Ca–O_x catalyst exhibits superior poison resistance.

INTRODUCTION

The catalyzed steam gasification of carbon solids such as graphite and chars has been quite extensively reported (*1–3*). This catalytic reaction is unusual because the gasification of the solid reactant occurs at a solid–solid (carbon–catalyst) interface. The reaction is used for production of gaseous fuels, the removal of polymeric carbon from oxide surfaces, and gasification of biomass (*4, 5*). There have been studies of the intermediates and the oxygenated surface species formed during carbon gasification (*6–11*).

We have previously described research using only potassium oxide as a catalyst for gasification (*12, 13*). We also found that potassium–nickel oxide mixtures exhibited markedly higher activity than that of either K_2O or NiO (*13*). In this paper, we introduce and describe the behavior of a superior poison-resistant catalyst mixture, potassium–calcium oxide, for the steam gasification of carbon solids. This catalyst exhibits high activity at relatively low temperatures (850–900 K) and it produces primarily H_2 and CO_2. The activity is at least partially attributable to the excellent wetting of carbon by the catalyst precursors in their molten state prior to their decomposition.

Electron microscopy studies indicate that a homogeneous binary catalyst is formed after decomposition of the nitrate precursor salts and that gasification occurs by edge recession of the graphite prismatic planes while the basal plane is unreactive. This is similar to findings with K–Ni–O catalysts (*14*). Water dissociation by the K–Ca–O_x catalyst was found to be an important reaction step. Hydrogen is released and oxygen forms compounds with the carbon. The rate-limiting step appears to be the breaking of C–C bonds releasing carbon oxides (*12*).

0021-9517/90 $3.00

The rate equation obtained for graphite gasification is given by

$$\text{Rate} = A' \exp(-209 \text{ kJ/mol}/RT)\, P^a(H_2O) \times P^b(H_2),$$

where $a \sim 0.5$ and $b \sim -0.2$ to -1. (The order of b for H_2 is catalyst dependent as shown in Table 2. It is -0.21 for K–Ca–O_x, -0.71 for K–O_x, and -1.04 for K–Ni–O_x.)

The rate is expressed in moles of carbon converted per mole of catalyst per second; $P(H_2O)$ is the water partial pressure, $P(H_2)$ represents hydrogen partial pressure, and a and b are the respective partial orders.

Chars from coals gasify at much higher rates (e.g., tenfold) than that of graphite. The relative ease of gasification of different types of carbon is lignite > subbituminous char > bituminous char > graphite and is independent of the catalyst used. The potassium–calcium oxide catalyst is much more resistant than the potassium–nickel oxide catalyst to poisoning either by the mineral content of the char or by sulfur artificially added to the sample.

EXPERIMENTAL

(A) *Sample Preparation*

Graphite was obtained from Ultra Carbon Corp. (spectroscopic grade Type UCP2; 325 mesh). Chars were obtained from the Institute of Gas Technology. Table 1 lists the relevant characteristics of the carbon sources tested. The samples were impregnated with nitrate solutions of potassium and nickel or of potassium and calcium to incipient wetness. The atomic ratio K/M^{+2} was kept equal to 1 and the ratio $K/C = 0.01$. The samples were dried at 420 K for 1 h.

(B) *Flow Reactor System (FRS)*

Figure 1 shows a diagram of the FRS used. The reactor is a 5-mm-i.d. alumina tube. About 0.5 g of sample is deposited between two alumina wool plugs. Steam is produced by pumping water with a Harvard compact infusion pump Model 975 through heated lines. By keeping water flows below 0.1 ml/min, the total pressure in the reactor is very close to 760 Torr. A liquid rate of 0.06 ml/min was selected as a standard flow, equivalent to 240 ml/min of steam at 850 K. Steam leaving the reactor is condensed by volume expansion. Gas flow produced is recorded by a precalibrated thermal mass flowmeter connected to a base time recorder and is analyzed by a gas chromatograph using a thermal conductivity detector and a carbosieve S-II 100/120 mesh 10 ft × $\frac{1}{8}$-in. column. The unit permits careful mass balancing, product analysis, and control of feed rates and temperature.

TABLE 1

Characteristics of Carbon Sources Used in this Work[a]

Carbon source	Ultimate analysis wt% (dry basis) (by diff)						Specific area (m^2/g) BET N_2
	C	H	S	N	O	ASH	
North Dakota char (lignite)	64.0	4.6	0.5	1.5	18.0	11.4	313
Rosebud char (subbituminous)	62.8	4.4	1.3	1.0	15.9	14.7	26.9
KY 13 char (bituminous)	73.7	4.8	1.4	1.9	10.1	8.1	10.1
Graphite	99.9	—	—	—	—	—	3

[a] Analysis supplied by IGT. Surface area measured by dynamic BET in this laboratory.

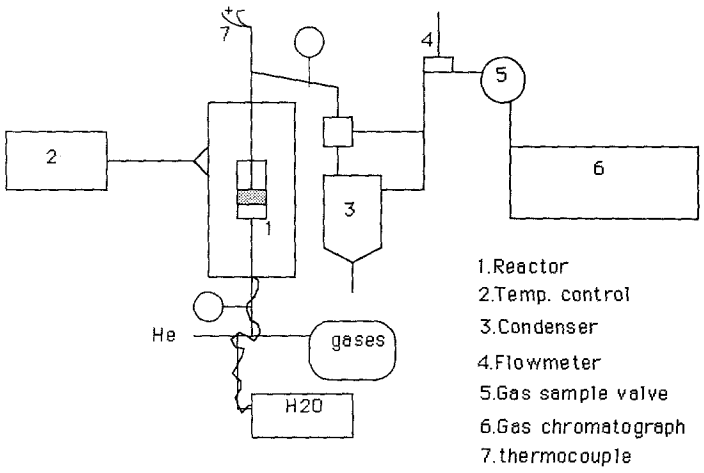

FIG. 1. Diagram of flow reactor system.

The sample treatment in the unit prior to steam gasification comprises an increase in temperature from ambient to the decomposition temperature (td) of the precursor salts plus 20 K at a rate of 12 K/min. This temperature is maintained for half an hour. The temperature is then raised to reaction temperature at a rate of 12 K/min for the K–Ca-containing samples or 2 K/min for the K–Ni-containing samples. A small He stream is maintained until 10 min after reaction temperature is reached in order to avoid air passing into the lines during the start of reaction.

(C) *Controlled Atmosphere Electron Microscopy (CAEM)*

Transparent flakes of graphite were prepared by attaching the graphite to a glass slide using low-melting-point wax and repeatedly cleaving the graphite along its basal plane with adhesive tape until only a small section was left stuck to the glass slide. The section was released using acetone, picked up on a gold 500-mesh grid, and allowed to dry in air. The graphite was then impregnated with K and Ca nitrate and the flow reactor system described was used to decompose the salts.

The experiments were performed in a KRATOS EM-1500 transmission electron microscope at the National Center for Electron Microscopy at the Lawrence Berkeley Laboratory.

A Gatan single-tilt heating stage was used in a Gatan environmental cell. Argon was bubbled through water and the water vapor/argon mixture was fed directly into the cell at a pressure of 3 Torr. The microscope was operated at its maximum accelerating voltage, 1.5 MeV, and dynamic images were displayed and recorded via a video camera.

RESULTS

(A) *Steam Gasification of Graphite—Kinetic Study*

The relative activities of various catalysts for gasification of graphite, a hydrocarbon-free carbon source, were studied.

Under constant conditions the main products of steam gasification are CO_2 and H_2, with small amounts of CO (<2%) and CH_4 (<0.5%). The selectivity to CO_2 (moles of CO_2 formed per mole of carbon converted) was always higher than 97% with a H_2/CO_2 ratio very close to 2. We therefore believe that the reaction occurring is

$$C + 2H_2O \rightarrow CO_2 + 2H_2.$$

Table 2 shows the rates and conversions reached after 700 min of reaction under

TABLE 2

Steam Gasification of Graphite with Various Catalysts

Catalyst	After 700 min of reaction under STD conditions		Kinetic study			
	Conversion %	Rate (mol/mol/min)	E_a (KJ/mol)	H_2O partial order (a)	H_2 partial order (b)	Regression (a)–(b)
K–O	15	0.091	265	0.66 ± 0.04	−0.71 ± 0.01	0.94–0.99
Ca–O	7	0.040	—	—	—	—
Ni–O	0	0.00	—	—	—	—
K–Ca–O	25	0.139	276	0.50 ± 0.03	−0.21 ± 0.01	0.96–0.98
K–Ni–O	28	0.145	273	0.69 ± 0.03	−1.04 ± 0.01	0.95–0.99

standard conditions (T = 893 K, FW = 0.066 ml/min, total P < 760 Torr, 0.5-g sample) for the bimetallic compounds studied and for the respective monometallics. K and Ca oxides by themselves show some activity under our experimental conditions; Ni oxide is inactive; increased activity is found with the metallic mixtures.

A kinetic study was performed to enhance the comparison between the two most active bimetallic catalysts of those studied for the steam gasification of the various carbon samples investigated. The partial orders of reaction were determined with graphite samples containing a catalyst/carbon molar ratio equal to 0.01 with a mole of catalyst comprising 1 mol of K and 1 mol of Ca or of Ni. The same determination was also made with a K/graphite sample having a catalyst/carbon molar ratio equal to 0.02. One of the reactants was diluted with inert gas (He), while keeping the partial pressure of the other gaseous reactants constant. Every system was kinetically tested after 30% of graphite conversion to ensure that a steady state was achieved (pseudo-zero order). Also, no tests were made after 70% conversion, so that major changes in catalyst/carbon ratio did not affect the final carbon conversion rates. These conditions required selection of different temperatures for each system: K–Ni/graphite, 933 K; K–Ca, 941 K; K/graphite, 953 K.

The high activation energies found for all the carbonaceous and catalyst samples studied in our system along with the very small grain size and the high linear velocity of the gases used indicate that chemical reaction steps are controlling the rate of reaction and not diffusion.

Most of the kinetic studies reported in the literature have been carried out in gravimetric systems in which the carbon conversion is monitored by weight loss. Because of the characteristics of this reaction (solid–solid and solid–gas reaction), care must be taken to perform kinetic studies in our flow reactor system as shown by Holstein (*15*). We therefore describe below in some detail how we analyzed our data.

During steady-state operation our reactor can be visualized as one in which a constant "flow" of carbon is passing through a stationary catalyst. If all other conditions are constant, including H_2O, H_2, and CO_2 partial pressures, the reaction rate should be constant. This state is experimentally observed with graphite and can be expressed because of our conditions (low water conversion levels, high space velocity) in a very simplified way as occurring in a differential reactor. Assuming that the number of moles of catalyst participating in the reaction is constant during the period of investigation one finds

$$R_c = (F_o/N_{cat})X \text{ or } R_c = SX, \qquad (1)$$

where R_c is the rate of carbon conversion per mole of catalyst, F_o is the "molar flow of carbon," N_{cat} indicates moles of catalyst

in the reactor, X indicates conversion, and S is the molar space velocity which under our conditions is approximately constant.

The rate expression can be generalized as

$$Rc = kf[P^a(H_2O)P^b(H_2). \ . \ .). \quad (2)$$

The partial orders of reaction can then be determined by varying the partial pressure of one component while keeping the partial pressures of the other components constant, using an inert gas to maintain the total pressure constant.

Under our conditions, CO_2 has been shown to have no effect on the reaction rate.

In the presence of a large excess of water or, alternatively, hydrogen, expression (2) becomes

$$Rc = k'P^a(H_2O) \quad \text{or} \quad Rc = k''P^b(H_2).$$

When the experimental data was plotted, good correlations were found, and the orders obtained for every system are presented in Table 2.

From these results it is apparent that the inhibiting effect of H_2 decreases in the order K–Ni > K > K–Ca. The close values of the activation energies indicate that the rate-controlling step may be independent of the catalysts. The high value found (about 60 Kcal/mol or 270 KJ/mol) indicates that the rate depends on a thermally activated step such as the surface complex decomposition suggested by Mims *et al.* (*8*).

(*B*) *Water Dissociation with K–CaO_x Catalyst*

When steam is passed over the K–Ca–O_x catalyst in the absence of carbon the dissociation of water is observed and the evolution of H_2 is readily detectable. The reaction stops after 2 h at 900 K when using 0.3 g of catalyst and steam at 1 atm. If the temperature is raised, an additional H_2 release is observed, but this always stops after a few minutes at each temperature. No release of O_2 was observed at any time. Blank checks without catalyst showed no H_2 release. H_2 release was observed for one cycle of increasing temperatures only. This is most likely due to the oxidation of the catalyst to a form that is no longer active for water dissociation as indicated by the absence of oxygen evolution. In the presence of carbon the water dissociation becomes catalytic, as the carbon provides a sink for the oxygen produced from H_2O thereby preventing the catalyst deactivation.

(*C*) *Controlled Atmosphere Electron Microscopy Studies of Graphite Gasification*

The entire process sequence from formation to reaction of the K–Ca oxide/graphite samples was followed by electron microscopy. Figure 2 shows the state of the sample before and Fig. 3 after decomposition of the salts at room temperature but before reaction. Good dispersion is observed after decomposition of the salts with a relatively wide distribution of particle sizes. The black areas are covered by catalyst, while the white background is due to carbon. A large and a small catalyst particle are denoted by A and B in Fig. 3.

Figures 4a and 4b show EDS electron micrograph analysis of particles of different sizes encircled as A and B in Fig. 3. The spectra are almost identical and apparently the metal oxide catalyst is thoroughly mixed, leading to the supposition that the catalyst activity is not due to an addition of individual activities but the result of a quite homogeneous combination of K and Ca.

The reaction in the electron microscope cell was initiated by heating to 853 K with a pure Ar stream (total P = 2 Torr). Once that temperature was reached, wet Ar was introduced at the same pressure. The temperature range explored under these conditions was 880 to 950 K. No visible reaction occurred until 893 K and 40 Torr of total pressure were reached. In Figs. 5, 6, 7, and 8 the progress of the reaction at 940 K is shown until all carbon in the focused area has been consumed as evidenced by no further movement over an extended time period (Fig. 8).

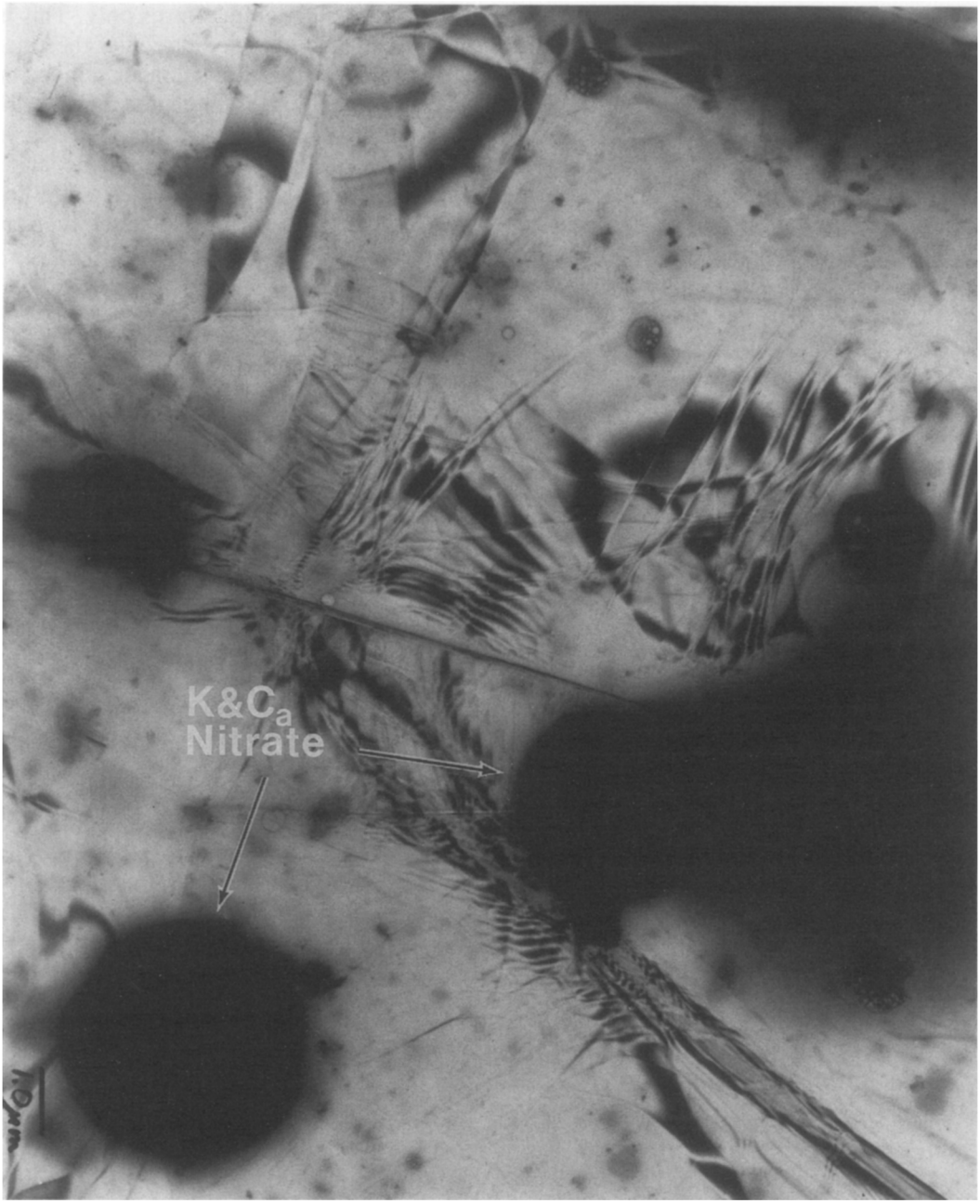

FIG. 2. Electron microscope picture of K–$Ca(NO_3)_3$/graphite on a gold grid.

Figure 5 shows an edge at the center with a dark band of catalyst in contact with it; this is in contrast with the particle distribution shown in Fig. 3. A catalyst spot on the basal plane is observed in the middle right side of the picture and at the extreme right can be noted a barely visible edge which appears clearly in Fig. 6 taken 1 min after Fig. 5. The left and right edges converge as gasification proceeds and finally merge.

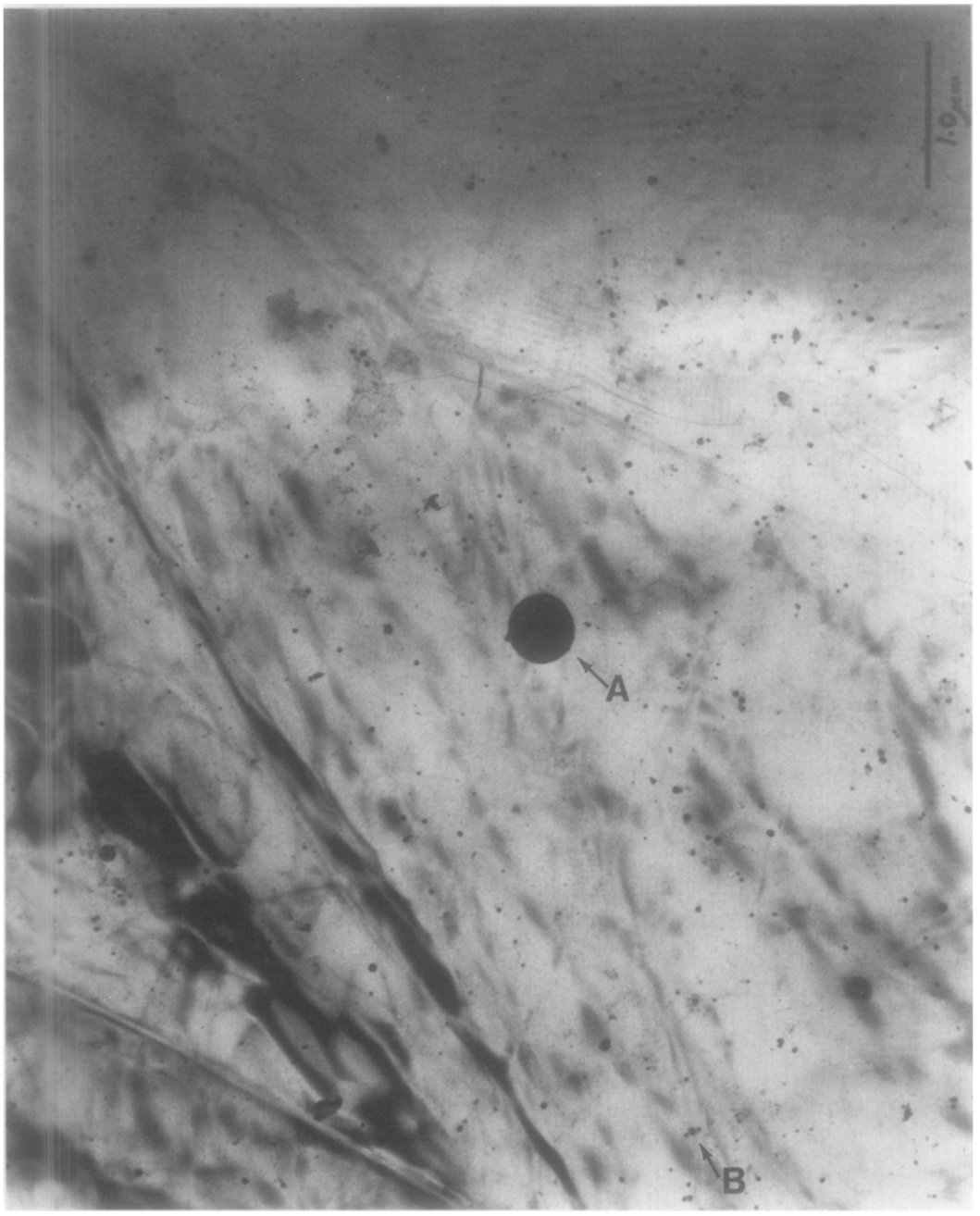

FIG. 3. Electron microscope picture of the sample of Fig. 2 after decomposition and before reaction.

The catalyst spot does not change until it is reached by the recession of the left edge (Fig. 7) as indicated by the diminishing distance between it and the large amount of catalyst in the center of the picture (Figs. 6 and 7). In Fig. 7 the catalyst spot has been incorporated into the larger catalyst area at the left edge. In any of the areas monitored at the different temperatures studied, no variations were observed for the catalyst

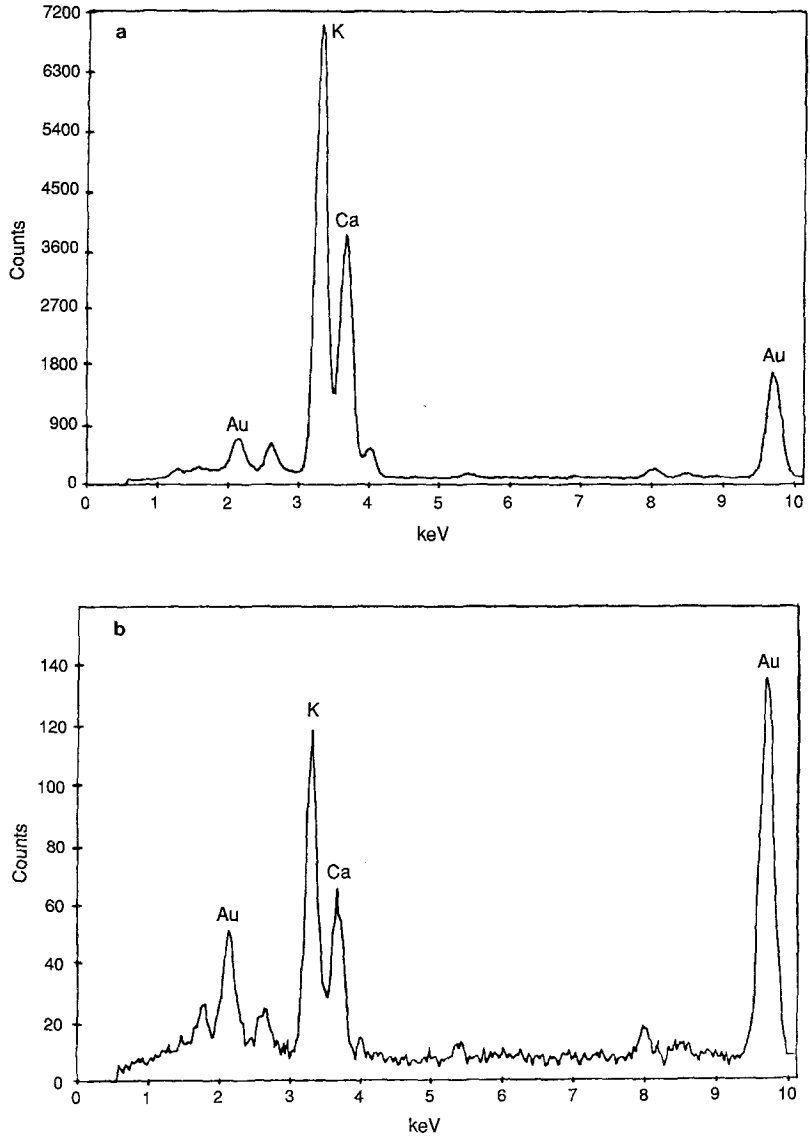

FIG. 4. (a) Electron micrograph of a big particle [A in Fig. 3] and (b) of a small particle [B in Fig. 3] showing homogeneous compositions of K and Ca.

spots deposited on the basal plane of graphite. Only edge recession was observed.

The reaction was completely stopped when a wet stream of Ar plus 6% H_2 was passed through the cell. Hydrogen inhibits the reaction as also shown by the kinetic studies.

The activation energy of the reaction with wet Ar has been calculated from four different temperatures and two different areas monitored. Figure 9 shows the Arrhenius plot giving an activation energy of 217 KJ or 52 Kcal/mol. This value is reasonably similar to that found in the flow reactor system.

(D) Char Gasification With Steam

Chars contain C–H bonds in addition to C–C bonds and have much higher surface areas than graphite. Since both the H/C ra-

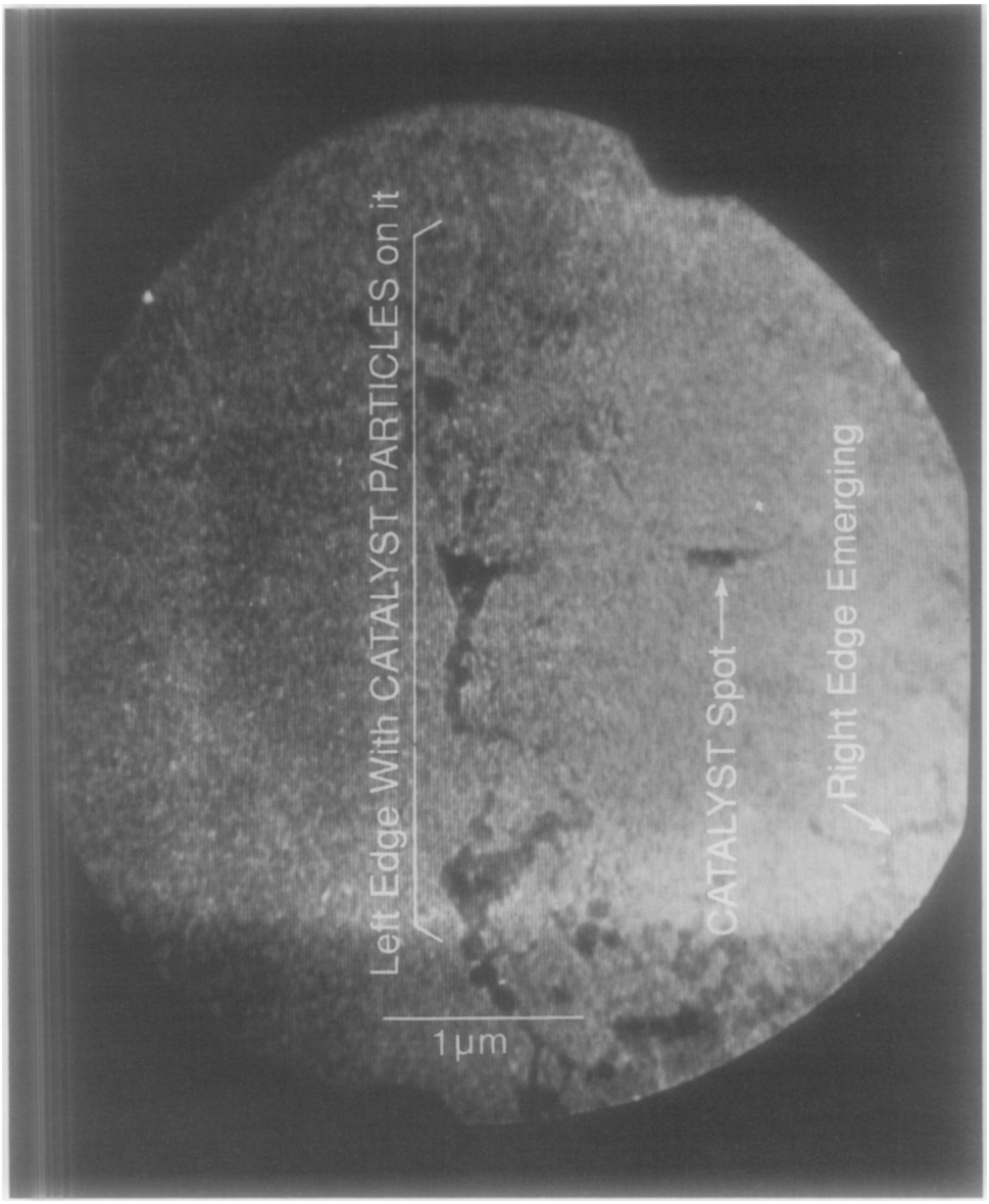

FIG. 5. State of a K–Ca$(O)_x$/graphite sample after 45 s reaction.

tio and the surface area (as well as mineral impurities content) vary from char to char, several different char types were investigated to establish the catalyst performance for their steam gasification. In Table 3 data for the K–Ca–O_x-catalyzed gasification of various chars are compared. The activation energies are similar to that of graphite, indicating that the much higher conversion and rates compared to those of graphite must be due to the char composition. The rate of gasification proceeds in the order lignite > subbituminous > bituminous > graphite. It should be noted that another mixed oxide,

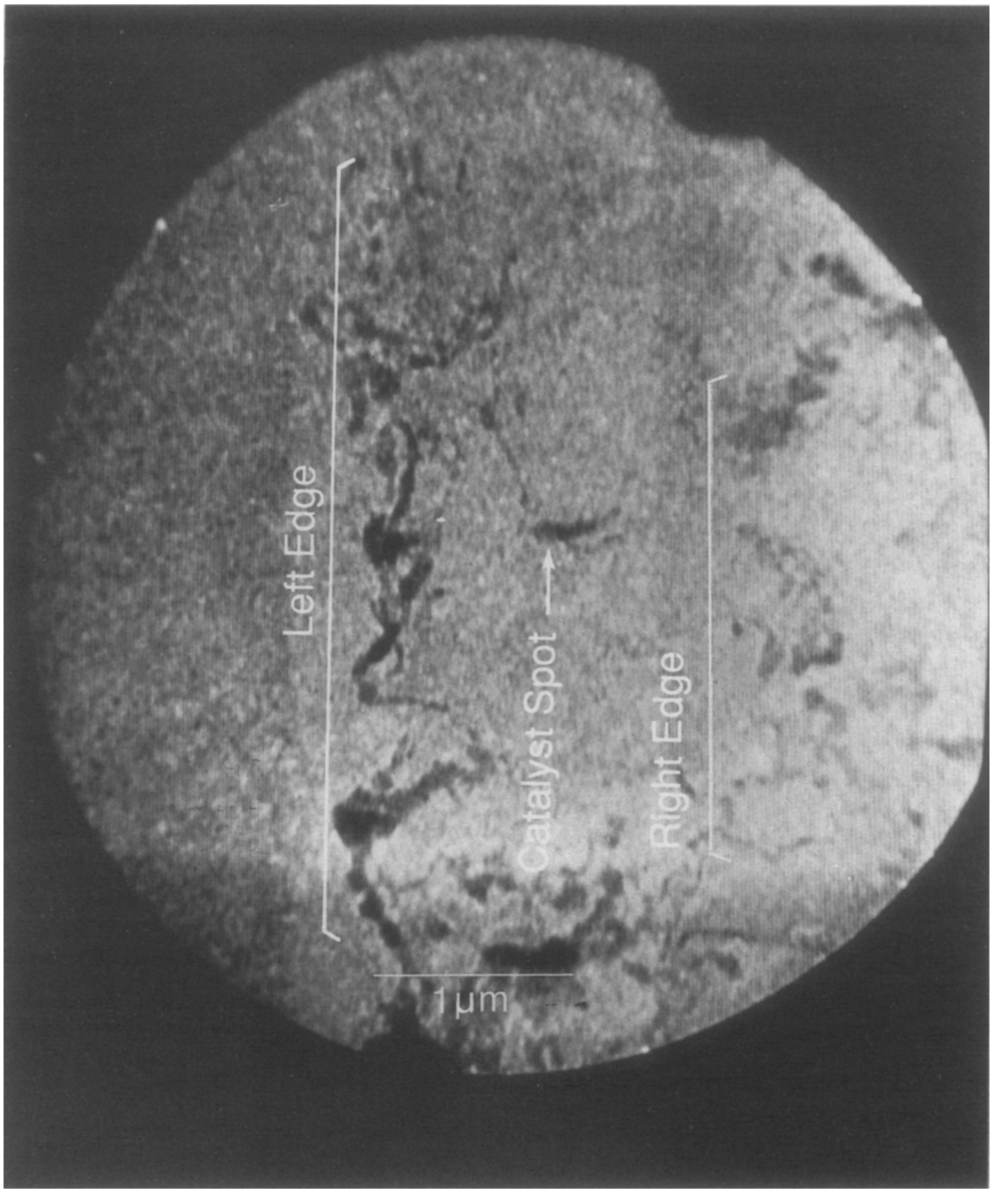

FIG. 6. Picture taken 1 min after Fig. 5. The progress of the left edge relative to the central catalyst spot of Fig. 5 can be observed and a second edge coming from the right side of the picture shows up more clearly.

K–Ni–O_x, exhibited identical trends when different chars were compared with graphite. Thus, the observed rate data is not a unique property of the K–Ca–O_x catalyst. The chars contain hydrocarbons that appear to gasify more rapidly than graphite. The reaction of steam with C–H bonds is more facile than the reaction with C–C bonds. In no case were hydrocarbons observed in the reaction products.

It was found that the K–Ca–O_x catalyst is highly resistant to poisoning by the sulfur content in the char. When K–Ni–O_x catalyst was used for steam gasification it was

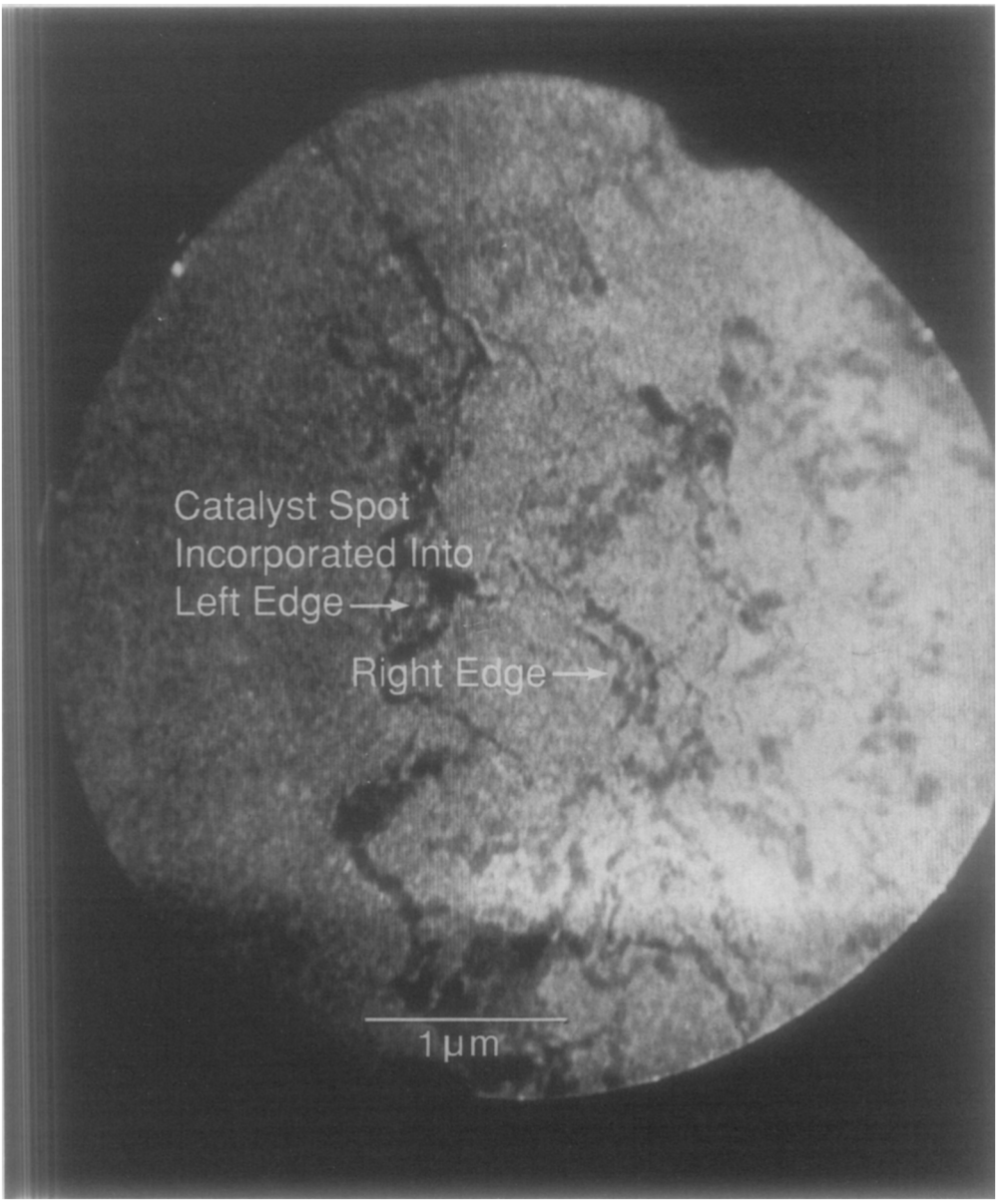

FIG. 7. Taken 3 min after Fig. 6. The central catalyst spot of Fig. 5 has been covered by the graphite edge progressing from the right side of the picture.

rapidly poisoned in the presence of sulfur.

Figure 10 compares the rates of steam gasification under the standard conditions of a demineralized char loaded with either K–Ca–O_x or K–Ni–O_x in the presence or absence of 3% sulfur (obtained by the decomposition of dibenzothiophene) to demonstrate the poison-resistant behavior exhibited by the K–Ca–O_x catalyst.

DISCUSSION

The K–Ca–O_x catalyst is much more active than potassium oxide or calcium oxide

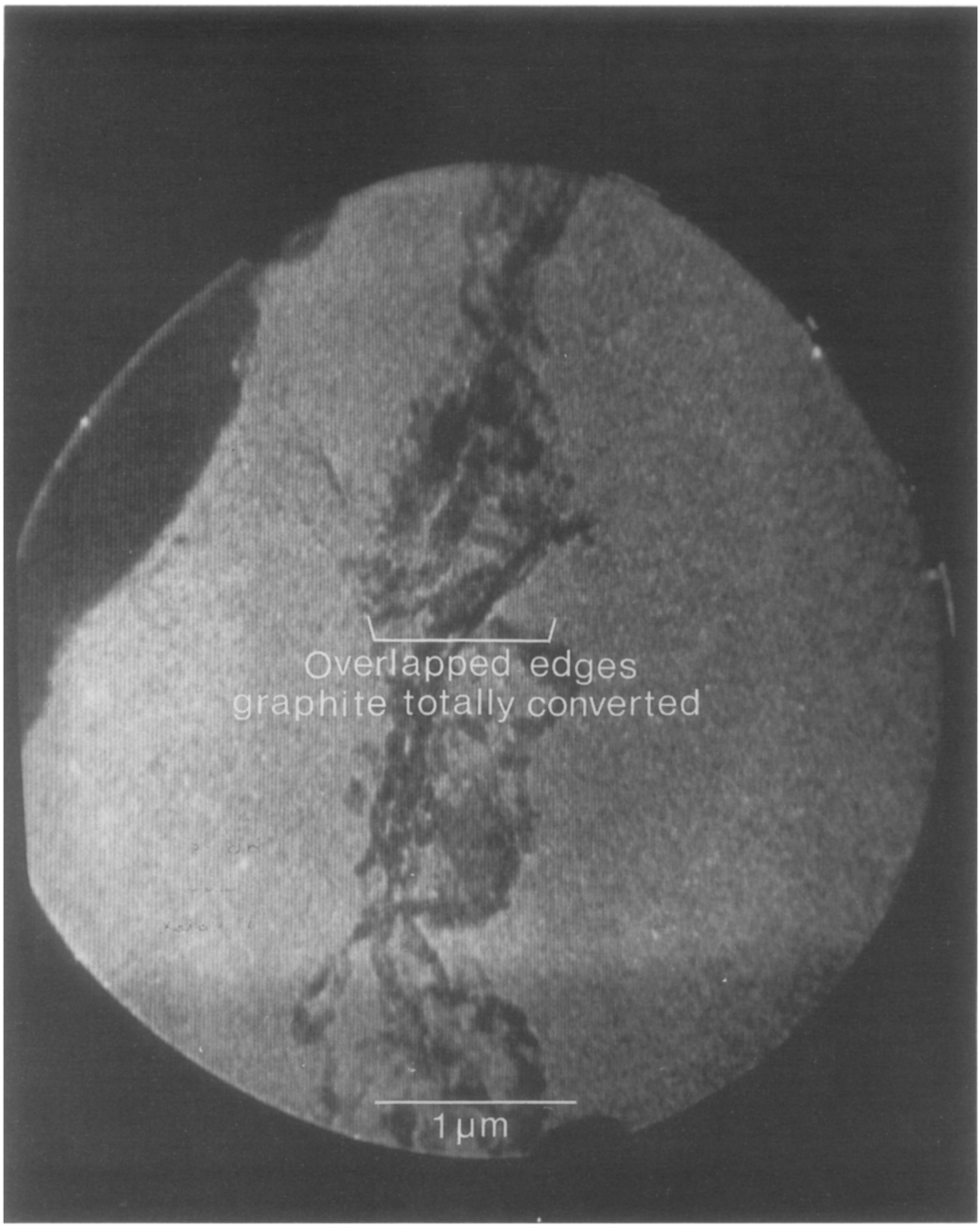

FIG. 8. Final view of the catalyst after all the graphite has been consumed.

alone as shown in Table 1. Its reaction rate is twice that of $K-O_x$ and fivefold that of $Ca-O_x$ at a temperature of 893 K and 750 Torr of steam. This high activity is probably due to the inhibition of a stable calcium carbonate formation that results in the case of calcium alone as a catalyst. In addition the formation of a molten eutectic phase which is observed during the catalyst preparation and prior to decomposition of the nitrate salts provides good wetting of the carbon solids.

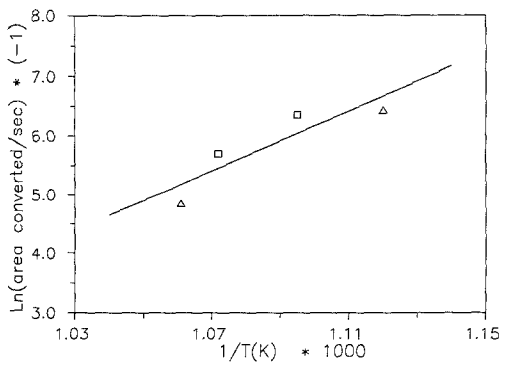

FIG. 9. Arrhenius plot for catalytic graphite gasification obtained by electron microscopy.

The rate equation for the gasification reaction and the activation energies for gasifying the various carbon solids (graphite and different chars) are very similar for different catalysts although the hydrogen inhibition effect varies somewhat from catalyst to catalyst, being the smallest for the K–Ca–O_x catalyst. Several oxygenated carbon species can coexist at the temperature range used in this work. However, the decomposition temperature for each of these species is different and the type of carbon oxide released can be different. Phenolic species decompose at temperatures higher than those used here and produce predominantly CO rather than CO_2. Under our conditions carboxylates and lactone species are decomposed, producing CO_2 (*11*).

It appears that the mechanism of gasification is very similar for the three catalysts. As suggested by earlier studies (*8, 12*), the C–C bond breaking next to a surface carbon–oxygen complex to produce CO_2 (or CO at higher temperatures) is the likely rate-determining step for carbon gasification. There is a great deal of supporting evidence for this model, including oxygen- and carbon-labeled isotope studies and temperature-programmed thermal desorption (*8, 12*). The formation of stable oxygenated surface species has been identified by spectroscopic techniques such as EPR, FTIR, and XPS (*10, 17, 18*). Also, the change in H_2/CO_2 ratio during steam gasification clearly indicates oxygen uptake by carbon in the beginning of the reaction (*16*).

The dissociation of water into hydrogen and oxygen by the catalyst has also been identified as an important reaction step. Surface science studies (*19, 20*) have shown the ability of potassium to dissociate water to produce K–O_x. It appears that the evolution of hydrogen derives from this process, as does the oxidation of carbon at the catalyst interface. Our results show that water dissociates by a stoichiometric reaction over the K–Ca–O_x catalyst. In the presence of carbon this reaction becomes catalytic and is an important step in the gasification although its activation energy is relatively low (138 KJ/mol or 33 Kcal/mol of H_2) (*13*).

Chars gasify at much higher rates than graphite (over tenfold increase, Table 3). It is clear that gasification of the carbons that contain many C–H bonds in addition to

TABLE 3

Steam Gasification of Three Chars with K–Ca–O Catalysts

Char (rank)	Activation energy (KJ/mol)	% Conversion after 120 min reaction	Reaction rate (mol/mol/min) 120 min	Selectivities			
				H_2	CO	CH_4	CO_2
North Dakota (lignite)	234	45	15.6	1.3	0.02	<0.006	0.975
Rosebud (subbituminous)	240	30	2.75	1.2	0.02	<0.005	0.975
KY 13 Frank. (bituminous)	269	15	0.82	0.98	0.1	<0.01	0.89

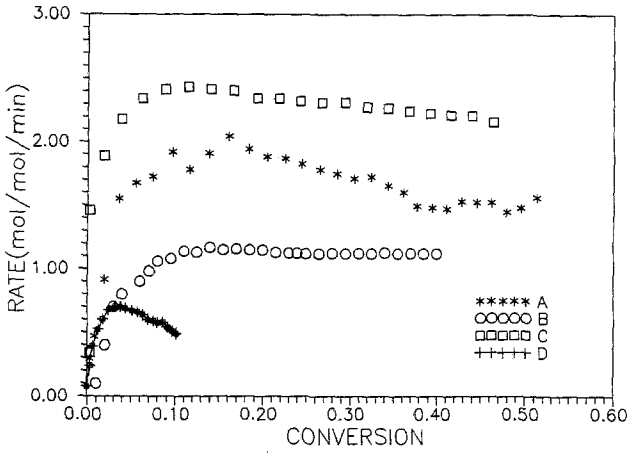

FIG. 10. Sulfur poisoning of demineralized K–Ni/KY 13 char and K–Ca/KY 13 char systems. Rate vs. conversion plots. (A) K–Ca/KY 13 char; (B) K–Ca/KY 13 char + 3%S (ex DBT); (C) K–Ni/KY 13 char; (D) K–Ni/KY 13 char + 3%S (ex DBT).

C–C bonds is more facile. This has the effect of increasing the rate without change in the activation energy for the process. Thus, it appears that the rate of gasification is the same for graphite and for chars but that the preexponential factor is greatly increased for chars. This could be related to the much higher edge density of chars. These are the sites from which gasification proceeds.

The K–Ca–O_x catalyst exhibits superior poison resistance compared to that of the K–Ni–O_x catalyst, which has similar steam gasification activity. This property should be of importance in the technology as it permits the use of carbon feedstocks that have not been demineralized or contain sulfur.

ACKNOWLEDGMENTS

The valuable assistance of S. Travis Palomares in this work is appreciated. This work was supported by the Assistant Secretary for Fossil Energy, Office of Management and Technical Coordination, Technical Division of the U.S. Department of Energy under Contract DE-AC03-SF00098, through the Morgantown Energy Technology Center, Morgantown, West Virginia 26505.

REFERENCES

1. Wood, B. J., and Sancier, E. M., *Catal. Rev. Sci. Eng.* **26,** 233 (1986).
2. Lang, R. J., *Proc. Fund. Catal. Coal Carbon Gas.* **86,** 23 (1986).
3. Wen, W.-Y., *Catal. Rev. Sci. Eng.* **22**(1) (1980).
4. Speight, J. G., "The Chemistry and Technology of Coal." Dekker, New York, 1983.
5. Wojciechowski, B. W., and Corma, A., "Catalytic Cracking." Dekker, New York, 1986.
6. Veraa, M. J., and Bell, A. T., *Fuel* **57,** 194 (1978).
7. McKee, D. W., and Chatterji, D., *Carbon* **13**(5), 381 (1975).
8. Mims, C. A., and Pabst, J. K., *Amer. Chem. Soc. Div. Fuel Chem.*, Preprint 25 (1980).
9. Kelemen, S. R., and Freund, H., *Carbon* **23,** 723 (1985).
10. Mims, C. A., and Pabst, J. K., *Proc. Int. Cong. Coal Sci. Dusseldorf,* 730 (1981).
11. Marchon, B., Carrazza, J., Heinemann, H., and Somorjai, G. A., *Carbon* **26,** 507 (1988).
12. Delanny, F., Tysoe, W. T., Heinemann, H., and Somorjai, G. A., *Appl. Catal.* **10** (1984).
13. Carrazza, J., Tysoe, W. T., Heinemann, H., and Somorjai, G. A., *J. Catal.* **96,** 234–241 (1985).
14. Carrazza, J., Chludzinsky, J. J., Heinemann, H., Somorjai, G. A., and Baker, R. T., *J. Catal.* **110,** 74 (1988).
15. Holstein, W. L., *Fuel* **62,** 259 (1983).
16. Heinemann, H., Somorjai, G. A., Pereira, P., and Carrazza, J., *ACS Div. Fuel Chem.* [preprint] **34**(1), 121 (1989).
17. Cerfontain, M. B., Kapteijn, F., and Moulijn, J. A., *in* "Proceedings, 8th International Congress on Catalysis, Berlin, 1984," Vol. 3, p. 593. Dechema, Frankfurt-am-Main, 1984.
18. Papirer, E., and Guyon, E., *Carbon* **16,** 127 (1978).
19. Thiel, P. A., Hrbek, J., de Paola, R. A., and Hoffman, F. M., *Chem. Phys. Lett.* **25,** 108 (1984).
20. Bonzel, H. P., Pirug, G., and Winkler, A., *Surf. Sci.* **175,** 287 (1986).